

Beamforming measurements of an axial fan in an industrial environment

Tamás Benedek, Péter Tóth

Received 2013-04-20, accepted 2013-06-30

Abstract

This paper summarizes a case study example on the methodology used for phased array microphone measurements in a realistic acoustic environment. A ducted fan rotor is measured in an environment, where structure born noise and aerodynamically generated noise cannot be separated using conventional single microphone acoustic analysis. The conditions of the measurement are similar to an industrial acoustic measurement scenario, where no acoustics treatment can be implemented for aiding in the source localization. The acoustics propagation paths are complex and combined with the high level of wind noise which the microphones exposed to, the interpretation of the results is difficult. The paper presents the processing and analyses of the many microphone worth of data of the phased array microphone system. The wind noise dominated cross spectral matrix is analyzed and source positions are obtained with beamforming procedures for both stationary and rotating sources.

Keywords

axial fan · phased array microphones · beamforming · rotating source model · industrial environment

1 Introduction

In recent years, acoustic analysis has become an important aspect of machine design and also of the evaluation of existing facilities, workshops or crowded community areas affected by noise. The goal of such an analysis is to seek possibilities for reducing the effect of noise on humans, which is enforced by new regulations or by the requirement of higher comfort levels [1, 2]. Almost always the most economical way to reduce the noise radiation is the decrease the strength of the noise sources. The identification of the strongest sound sources is a key problem to be solved for obtaining quieter machines. In analyzing existing facilities the identification procedure can be aided by phased array microphones [3].

In industrial environments the noise is often caused by a ventilation system, composed the high speed turbulent flow generated noise and mechanical originated noise, such as the vibrating elements of the machine [4]. Beamforming techniques provide a unique means for i) the identification of dominant noise sources, ii) making a distinction between rotor-originated noise and other noise components [5]. These features help to extend the possibilities of the presently used measuring instrumentation for use in the acoustic diagnostics of machines.

In an acoustic diagnostics measurement the beamforming method should be able to identify the most important source mechanisms quickly, without significant modification of the original industrial apparatus. The laboratory modeling of an industrial environment is usually difficult or not possible at all, due to the insufficient information regarding the source strength and directivity. Because of the coexistence of many sources, acoustic measurements with a single microphone do not allow the precise characterization of the directivity and source strength of the sources, and therefore at far-field locations the dominant acoustic sources cannot be easily identified. In these cases the phased array microphone system could have an important diagnostic use.

Turbomachine beamforming measurements found in the literature are usually laboratory tests. In reference [6] tonal noise components of a turbofan engine were investigated and it was found that installation effects of the inflow control device alter

Tamás Benedek

Department of Fluid Mechanics Budapest University of Technology and Economics, H-1111 Budapest, Bertalan Lajos utca 4-6, Hungary
e-mail: benedek@ara.bme.hu

Péter Tóth

Department of Fluid Mechanics Budapest University of Technology and Economics, H-1111 Budapest, Bertalan Lajos utca 4-6, Hungary
e-mail: toth@ara.bme.hu

the results, showing that the measurement set-up of full scale measurements can lead to the necessity of careful interpretation of the results.

Ducted fan measurements to retrieve the rotating broadband sources of the rotor using an inversion technique are presented in [7]. The method is an extension of the identification of stationary in duct monopoles by utilizing the duct modes presented in [8]. Wall mounted microphones are used, and it was found that accurate measurements require an array to be closer than 0.1 wavelengths to the rotor. Therefore the method requires access to and preparation of the duct close to the rotor.

Measurements of turbofans are presented in [9]. It was found that by using conventional and rotating source beamforming techniques, it is possible to identify noise sources on the rotating blades as well as on the outlet guide vane. For axisymmetric problems a circular harmonics beamforming technique is proposed in [10], which can easily be extended to rotating sources, giving an alternative to [5, 9]. The method requires a circular microphone array mounted into the duct wall.

The mentioned examples are common, in the sense that turbomachines were measured, but in a laboratory environment. These laboratory tests presented the feasibility of fan noise investigations using beamforming techniques and also discussed some important implementation issues. None of the tests show the feasibility of measurements in a complex measurement environment such as an industrial environment. It is anticipated that the out of laboratory measurement with microphone arrays does not have a well-established methodology, as of yet.

On-site measurements usually have special circumstances, which should be accounted for the duration of the measurement. These can be the high level background noise or the constraints on the location of the microphone array imposed by the available space, the acoustic transparency between the rotor and the array and the high level of hydrodynamic noise over the microphone array. Even with the use of robust beamforming methods these circumstances can prohibit the interpretation of the results.

In this study, a general purpose phased array microphone system is used for the beamforming of rotating and non-rotating sources of an axial fan operating in confined industrial environment. This is a representative configuration for induced-flow industrial or building ventilation systems, in which the noise can propagate in the suction duct. As an inevitable compromise in instrumentation of the ad hoc on-site measurement, the microphone array has been set up in the duct. The case study has been designed to survey the limits and required improvements necessary for applying beamforming technique in real-life industrial fan application. Source maps will be presented and analyzed, considering the issues related to the processing techniques, and giving an application oriented view of the problems that one would face in similar industrial measurement situations.

2 Beamforming

Phased array microphone systems operate on the basis of the beamforming methodology [11], where the phase difference between the signals of multiple microphones is utilized to estimate the direction of arrival of the wave front. The concept is illustrated in Fig. 1 for plane wave direction identification using a linear microphone array. By adjusting the phase shift (time delays) of the microphones signals relative to each other, a maximum correlation between them can be obtained. The corresponding phase shifts (time delays) are representative of the direction Θ (Fig. 1) of the incident wave. This beamforming method is called the Delay & Sum (DS) method [3]. The method can be considered as forming a sensitivity curve, called mainlobe that can be directed toward the source by phase (time delay) adjustments. Plane waves, monopoles or higher order acoustic sources can be localized by accounting for their source character in the calculation of the microphones phase shifts. Possible source positions can be defined providing focus points for the beamforming methodology. Beamforming maps display the strength of the model sources.

In the present paper, two types of beamforming algorithm are used. One method is the presented DS. The other is an extension of the DS method for rotating source models called Rotating Source Identifier (ROSI) [5]. Both methods are assuming monopole point sources at the focus points, radiating spherical waves into the free space.

The methods use the cross-spectral matrix of the microphone signals to represent the phase and amplitude of the measured acoustic signals. The cross-spectral matrix, \mathbf{C} , is created by an averaging procedure, for a given circular frequency ω and all microphone combinations. The measured discrete time data of the microphones are divided into equal segments, and Fourier transforms are computed. Then the averaged cross spectral matrix is computed from signals $y_m^v(\omega)$ which is the v^{th} section of Fourier transformed signal for microphone m . The cross spectral matrix component m, n can be written as:

$$C_{mm}(\omega) = \frac{1}{V} \sum y_m^v(\omega) y_m^{v\dagger}(\omega)$$

If the number of microphones are denoted by M then $m = 1 \dots M$, $n = 1 \dots M$. the complex conjugate transpose is denoted by \dagger . The averaging of the V segments of data helps to decrease the contribution of the uncorrelated random noise when $m \neq n$. On the other hand the averaging of the cross-spectral matrix elements does not decrease the effect of the uncorrelated noise of the auto spectrum (when $m = n$) [3]. This has an important implication concerning the beamforming of noisy signals, and leads to the concept of the diagonal removal algorithm (DR), where the auto spectral components of \mathbf{C} are removed, in order to increase the dynamic range of the beamforming map [5]. The effect of the diagonal removal method depends on the measured data itself. In some cases it results in non-physical source strengths [8]. The removal of the diagonal significantly decreases the level

of the source map when the acoustics sources to be measured are weak compared to the spatially uncorrelated noise sources. At very high background noise levels, it was found in [14] that the DR method is not effective in reducing the beamforming error. In extreme cases, if there is no measurable correlation between the microphone signals, the source strengths of the beamforming, the output with DR algorithm will be zero and a uniform constant value across the source map without DR method. Therefore the difference of sound amplitudes on the beamforming map without or with the diagonal removal reflects the level of the uncorrelated data in \mathbf{C} . If the difference is high there is a chance that small level acoustic sources are lost due to high incoherent noise at the frequency of interest.

An important aspect of the source maps is the existence of the ghost sources or sidelobes due to the finite number of microphones and finite size of the array [12]. These sidelobes are local correlation peaks on the source maps at positions where no physical sources exist. Their characteristics are related to the array geometry and processing algorithms. From a practical point of view these sidelobes always exist to a certain extent, and make it difficult to interpret the source maps. Previous investigations of the applied array in an anechoic chamber showed that the sidelobe levels are about 6-7 dB below the maximum source amplitude. Therefore in this paper we plot the beamforming maps to represent maximum range of 5 dB in order to exclude the sidelobes of the highest peak.

The beamforming algorithm has a limited capability to distinguish the individual sound sources spatially. This resolution limit of the used algorithm can be theoretically estimated. The resolution d is defined as the mainlobe width at the -3dB point. This limit can be estimated in the same way as the diffraction limit of finite aperture imaging systems [11].

$$d = 1.22 \frac{Zc}{Df},$$

where c is the speed of sound D is the diameter of the array, Z is the distance of the source from the array and $f = \omega/2\pi$ is the frequency of interest

The other method used in this paper is the ROSI method. It corrects the time differences and amplitudes between the model source point and the receiver by accounting for the position and velocity of the sources. The correction procedure is the following. If the time series data of microphone m is denoted by $\hat{y}_m(t_m)$ then the source signal $\hat{\sigma}_s(t)$ can be computed as

$$\hat{\sigma}_s(t) = \frac{\hat{y}_m(t_m)}{T_m(t_m, t)}$$

where

$$T_m(t_m, t) = \frac{1}{4\pi c \left(t_m - t - \frac{1}{c^2} Q \right)}$$

$$Q = \mathbf{x}'_s(t) \cdot [\mathbf{x}_m - \mathbf{x}_s(t)]$$

The position vector of the model monopole source s is \mathbf{x}_s . The velocity vector of the source is $\mathbf{x}'_s(t)$, and the dot denotes a scalar

product. The time t_m of the microphone signal m can be computed as:

$$t_m = t + \frac{|\mathbf{x}_m - \mathbf{x}_s(t)|}{c}$$

In order to have the same uniform time discretization of the computed source signal $\hat{\sigma}_s(t)$ for each microphone m , the signals have to be interpolated. These corrected source signals are used to compute the cross-spectral matrix of the array and the DS method (already having delayed signals for position s) is applied. The previously mentioned diagonal removal algorithm can also be used in the ROSI algorithm in the same manner described above. As the computation needs the source position as a function of time, a movement tracking signal indicating the shaft position has to be also recorded, and the source positions computed accordingly. The required computational resources for this implementation of the ROSI method are significantly higher compared to the DS beamforming method. The time for calculating the strength of the same number of model points is about two orders of magnitude higher when the ROSI algorithm is used. For a more detailed description of the ROSI method consult reference [5].

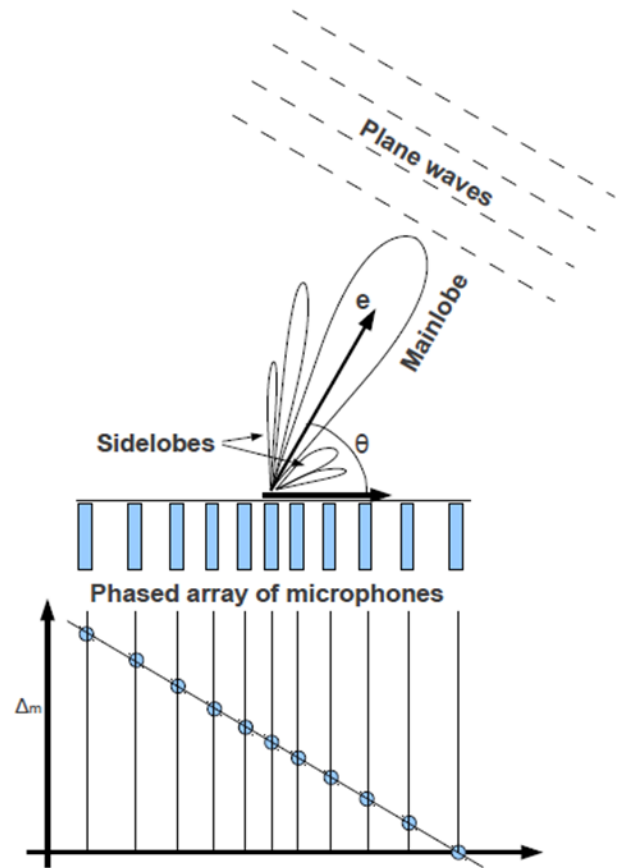


Fig. 1. The concept of DS beamforming using a linear array of microphones.

3 The measurement setup

The measurement was made in the low-speed wind-tunnel of the Hungarian Institute of Agricultural Engineering of Gödöllő. The environment can be described as an industrial environment,

not ideal for acoustic measurements (Fig. 3). A schematic picture of the tunnel and the measurement setup can be seen on Fig. 3. The fan (Fig. 2) was designed at the Department of Fluid Mechanics (DFM). The rotor blades are forward skewed and designed according to the controlled vortex design method. The fan is belt driven by an electric motor equipped with a frequency inverter. Downstream of the rotor there is a stator section and in front of the rotor a half-spherical nose cone is mounted on three supports. An adjustable plane diffuser, located at the outlet of the tunnel, can be used in order to set the operating point. The windtunnel has a rectangular cross-section and before the fan there is a transition element from rectangular to circular. The important data of the fan can be seen in Tab. 1 and an aerodynamic description of the fan can be found in reference [15].



Fig. 2. The windtunnel and the fan

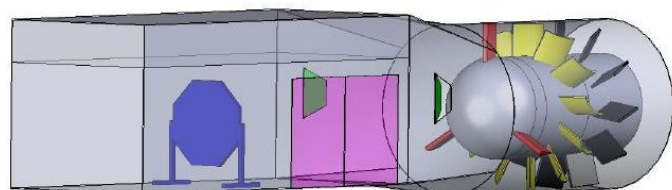


Fig. 3. The measurement configuration

The phased array measurements were performed with the general purpose Optinav Inc., Array 24 phased array system. DFM is in possession of the array. The microphones of the array arranged along a logarithmic spiral curve on the surface of an octagonal aluminum plate. The array was designed to have a high rejection of sidelobes in the widest possible frequency range. The microphone positions are guaranteed by precise manufacturing of the aluminum plate. During the measurement of the rotor noise, the first microphone channel was used to synchronously acquire the index signal emitted by an optical encoder at every rotor revolution. This signal was required for synchronization of the acoustic model with the rotor position when the ROSI algorithm was used. In this way, 23 microphones of the array were used to obtain the acoustic data. Tab. 1 also includes the data of the array.

The array was placed in the wind tunnel, upstream of the door of the measurement section. The placement was highly constrained by the points available for fixing the array to the tunnel wall as well as by the flow conditions. The array distance from the rotor was five times the diameter of the array, to com-

promise between a good resolution and the disturbing effect of the array separation bubble on the rotor flow. For this same reason the bypass doors on the sidewalls were also opened as well. (The doors are marked with green on Fig. 3, and can be seen in a closed position in Fig. 2) The plane of the array was adjusted approximately parallel to the plane of the rotor.

Since the array is in the flow, hydrodynamic pressure fluctuations have an important effect on the microphone signals. In order to reduce this effect, memory foam was mounted on the array surface, which can decrease the direct hydrodynamic pressure fluctuations, on the microphones [16]. The damping effect of the foam on the acoustic fluctuations was measured for frequency bands with bandwidth of 86 Hz and interpolated for each frequency in order to compensate the results.

The design operating conditions were set with the help of the plane diffuser. The measurement was made at two different rotational speeds. In Tab. 2 can be found the information about the measurement setups.

The measurement aimed at identifying the dominant noise sources in the measurement section of the wind tunnel. The fan rotor was expected to emit the most significant noise because this element delivers the momentum to the flow. Besides this, further noise sources such as vibrating tunnel sidewalls were expected. The separation of these sources is attempted herein by using various beamforming techniques.

Tab. 1. Data of the fan and array

Rotor diameter	2 m
Hub to tip ratio	0.6
Blade number of the rotor	12
Blade number of the stator	11
Size of the upstream duct	2 m x 1.5 m
Sampling frequency	44100 Hz
Bits per sample	24
Diameter of the array	0.95 m
Number of microphones	23

Tab. 2. Data of the measurement configurations

	Low speed	High speed
Array distance from the rotor	~5 m	~5 m
Number of revolution	277 1/min	416 1/min
Blade passing frequency	55.4 Hz	83.2 Hz
Rotor-stator interaction frequency	609.4 Hz	915.2 Hz

4 Array calibration and uncertainty

The beamforming maps are normalized in such a way that the maximum of the source corresponds to the sound pressure level which would be observed at the position of the array, if only that particular source existed.

The array system was previously calibrated in the George von Békésy Acoustic Research Laboratory, operated by DFM. This

amplitude calibration was done by measuring a point source with the array and comparing the spectrum of the peak on the beamforming map with the spectrum of a reference microphone placed at the center of the array [12]. The array was removed when the reference microphone spectrum was measured. The signal to noise ratio during the calibration was higher than 10 in the investigated frequency range. The uncertainty of the reference microphone calibration was 0.3 dB given by the manufacturer of the microphone calibrator. The calibration of the array was repeated three times, but the array and reference microphone position was not changed. The calibration factors were within 0.1 dB of the mean in each one-third octave band. It was found that the acoustic levels of the beamforming map have some angular dependence, meaning that the measured sound pressure level of the same source varies, depending on its location on the beamforming map. The used calibration factors cannot account for this angular dependence, therefore this is included as an additional uncertainty of the source levels. It is estimated that this uncertainty is 0.1 dB in the 15° half cone angle from the array axis. The estimated uncertainties of the beamforming maps are calculated for a worst case situation by adding together the above bounds giving 0.5 dB uncertainty. The reference microphone calibration uncertainty and the uncertainty related to the repeatability shift the levels of the source maps. It is also known that the source coherence and negative sidelobes can affect the measured source amplitude values [17]. Which means that the absolute levels of the source map amplitudes can have higher uncertainties, and are not to be used for the evaluation of the machine. On the other hand these uncertainties do not affect the comparability of the sources on the same source map, only the uncertainty from the angle dependence of the source amplitude affects this comparison.

It is important that for reliable measurements it is required to have an acceptable level of dynamic range of the source map. This dynamic range of the source maps is related to the sidelobes of the beamforming method. The sidelobes are the ghost sources of the original source generated by the aliasing effect, and can be visible on the source maps. These ghost sources do not represent any physical sound source, but they are an artifact of the beamforming. It is often attempted to lower the level of the sidelobes as much as possible by array design and modified processing methods.

The distinction of the sidelobes and the true sources can be hard to see whenever many physical sources co-exist on the beamforming map. One guiding idea in such cases is to determine the sidelobe levels in response to one measured source. The ratio of the mainlobe (true source) level to the maximum sidelobe level is the mainlobe to sidelobe ratio (MSR) of the array. The MSR value of the array is frequency dependent and in case of the used array the manufacturer suggests to use 5-7dB dynamic range. In order to safely suppress the sidelobes in this study the dynamic range is chosen to be 5dB. Even if such general rules exist for dealing with sidelobes [12], the given mea-

surement data always needs to be carefully examined and interpreted, which makes the use of the phased array data non-trivial. It will be seen in the next sections that beamforming maps of noisy microphone signals can lead to a dB range of only few dB on the source plots and the use of the DR algorithm, or other source models, such as ROSI, is promoted in order to be able to describe acoustic sources in a combined evaluation approach of several beamforming maps.

The ROSI algorithm requires the specification of the center of rotation of the model sources. The accuracy of the definition of this center can influence the results. The measurement of this center position is based on the picture recorded from the array. While the calibration of the camera picture with the source location is obtained in the anechoic chamber, the determination of the alignment of the array with other parts of the measurement set-up can be difficult. In the presented case, the center of the nose cone can be identified on the picture and this point is assigned as the center of rotation. However, the rotor center point is behind the nose cone by approximately 1.5 m. If the array center line is not perfectly aligned with the rotor axis, the center of the nose can be at a slightly different position in the picture than the real center of the rotor (i.e. the perspective of the photo causes some inaccuracy). An estimated upper limit for such an error in the present configuration is approximately 0.1 m. Previous numerical simulations showed that this level of error slightly blurs the source map, but individual sources can still be identified. The measurement source levels are also changed by the misalignment of the center. The numerical simulation showed that a 0.1m error in the center position causes -0.5 dB change in the absolute level of the source map. This also causes 0.3 dB difference between the source amplitudes those would be at equal level without the center position error. This level of errors considered to be small if the dynamic ranges of the maps are the suggested 5 dB. Consequently, the reduction of this uncertainty was not considered necessary.

Concerning the implementations of our in-house DS and ROSI algorithms they should give the same result when the rotation speed of the sources is set to zero and also the rotation speed set to zero in the ROSI algorithm. The mathematical formulation of the ROSI algorithm then gives the same result as the DS and this has to be reflected by the implemented program code as well. This is verified and it is found that the two methods gives the same results, the maximum and the range of the scales of the source maps are different only by a fraction of a decibel, which is due to the different processing methodologies of the algorithms. The implementation of the methods is therefore consistent.

5 Results

5.1 Spectral Analysis

Prior to the analysis of the beamforming maps the auto spectra of the microphones are first investigated. The averaged Sound Pressure Level Spectrum L of the 23 array microphones is used

for this investigation

$$L = 20 \log_{10} \left(\frac{\sqrt{\frac{1}{M} \sum_{m=1}^M C_{mm}}}{\Delta f p_{ref}} \right)$$

where C_{mm} are the diagonal elements of \mathbf{C} ($m = 1..M$) and $p_{ref} = 2 \times 10^{-5}$ Pa. The presented results are computed by a 16384 point FFT and the recorded time signal is divided into V segments (see. Sec. 2) with 50 % overlaps. The number of averaged segments, V , depends on the acquisition time, T_a . The frequency resolution is $\Delta f = 2.65 \text{ Hz}$.

For the characterization of the effect of averaging time on the auto spectra, the standard deviation is used. It is important to note that by increasing the averaging interval, the main levels of the spectra do not change significantly. The standard deviation of the difference between these successive spectra can be used to define a minimum averaging length. This standard deviation is presented in Tab. 1. Averaging across a frequency range is denoted by $\langle \dots \rangle$. When the averaging time is higher than 10 s, the change of the standard deviation is weak between successive steps. Therefore, for the auto spectra, $T_a = 10$ s (corresponding to 46 rotor revolutions at 277 rpm) is recommended as the minimum sampling time for the computation of the spectra.

With regard to the beamforming procedure, it is more important to investigate the beamforming spectra that contain the cross spectral components of \mathbf{C} . The beamforming spectrum L' is the spectrum of the highest peak on the beamforming maps. Comparing these beamforming spectra in Fig. 4, one can see that the mean value of the beamforming spectrum is decreasing when increasing the averaging time. This is contrary to the auto spectra, where the mean is not changing much in this averaging procedure. It is also interesting that this decrease is not constant over the frequency range, but is lower at lower frequencies and higher at higher frequencies. Therefore, the quantitative comparison in Tab. 2 is split into two frequency ranges at 2 kHz. In this table the mean of the difference of the successive spectra are depicted when the averaging interval is increased. The following trends can be observed in Fig. 4. The differences below 2 kHz are systematically smaller than those above 2 kHz. The averaging interval can only be chosen by considering frequencies above 2 KHz. The beamforming spectrum is not changing significantly for an averaging time greater than 10 s. Considering that the computational cost of the ROSI algorithm is increasing with the interval of the data, $T_a = 10$ s is utilized for the following calculations. This 10 s corresponds to 46 rotor revolutions at 277 rpm.

If the flow speed is changed, one can observe that the sound pressure level is changing by approximately the same level at every frequency. This is suggesting that the physical phenomenon generating all dominant spectral components is the same, and related either to the flow noise or to the acoustics radiation inside the wind tunnel. It is likely that at lower frequencies the effects of the hydrodynamic fluctuations of the flow dominate the array spectra, and due to the mentioned constant amplitude

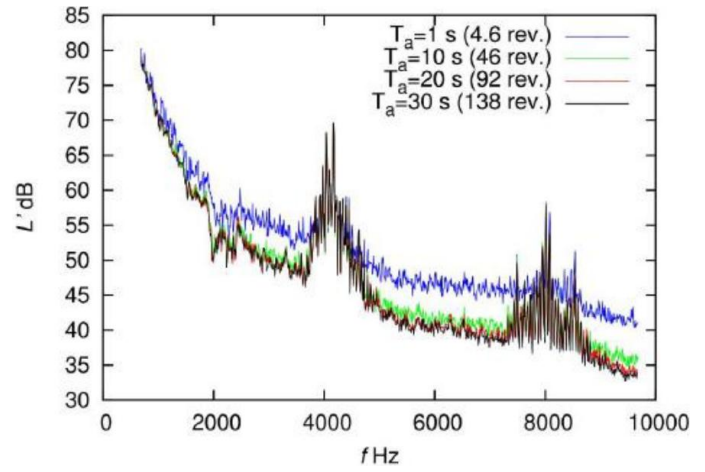


Fig. 4. The spectrum of the maximum of the beamforming map, for different length time signals.

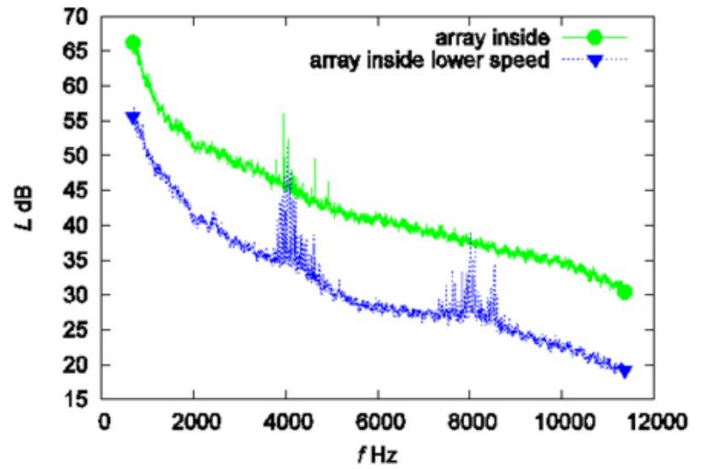


Fig. 5. Averaged spectra of the microphone array for various revolution speeds.

Tab. 3. The effect of averaging time on the auto spectra

Auto spectra	
T_a^i, T_a^{i+1}	$\sqrt{\langle (L^i - L^{i+1})^2 \rangle}_{0.7 \div 11 \text{ kHz}}}$
1 s, 10 s	2.2 dB
10 s, 20 s	0.4 dB
20 s, 30s	0.3 dB

Tab. 4. The effect of averaging time on beamforming spectra L'

Beamforming spectrum		
$T_a^i T_a^{i+1}$	$\langle L^i - L^{i+1} \rangle_{0.7 \div 2 \text{ kHz}}$	$\langle L^i - L^{i+1} \rangle_{2 \div 11 \text{ kHz}}$
1 s, 10 s	2.2 dB	4.1 dB
10 s, 20 s	0.2 dB	0.7 dB
20 s, 30 s	0.01 dB	0.3 dB

scaling in the frequency band, the same physical phenomenon is dominant at higher frequencies. This is foreshadowing the difficulty of identifying sound sources based on the recorded microphone data. The effect is connected to the previous analysis of the cross-spectra, where the cross-spectra levels need a certain minimum averaging time to settle down.

Fig. 5 shows the measured spectrums at different revolution speeds. The spectrum contains tonal noise components around 4 kHz and 8 kHz. These tonal components are not present when the wind tunnel is switched off. Their amplitude is changing slightly with flow velocity but their frequency is not. Considering the rotor blade passing and interaction frequencies mentioned in Sec. 3, no significant noise components are expected in this frequency range, however, an explanation for these higher frequency tonal noise sources could be vortex blade interaction noise if the three nose cone pillars generate von Kármán Vortex Street. The interaction frequency of these vortices with the rotor can be estimated by assuming a Strouhal-number of 0.2, an annular flow velocity of 13 m/s and rib diameter 0.05 m. The vortex shedding frequency is then ~ 52 Hz, which gives an interaction frequency of ~ 3000 Hz at 277 rpm. This shows the possibility for higher frequency aeroacoustic tonal noise generation by the machine. This tonal component, however would significantly scale with the flow velocity, which is not observed on the spectrum, and consequently the tonal components have a different origin. This is suggesting that they are not related to aeroacoustic noise sources, but possibly have an electrical nature, originating from the wind tunnel electric motor or controller unit. This argument shows the importance of measurements at various machine speeds, hence enabling the verification of the scaling laws, and also the identification of certain acoustic phenomena with a simple theoretical calculation.

As a consequence of the spectral analyses, we will focus only on broadband noise source identification in the following sections, where aeroacoustic sources are investigated. The frequency bandwidths of the beamforming maps will be one-third octave bands. The one-third octave band analysis is a standard for broadband acoustic analysis. It allows the identification of the sources at various positions, while keeping the number of source maps to a minimal.

The frequency range of 2.8-7 kHz is chosen for the following investigations, which is especially sensitive from the viewpoint of human audition. Another reason behind the lower limit is the poor resolution of the array (see Sec. 2.), while the higher limits because many individual source spots appear on the maps at frequencies higher than 7 kHz which is hard to evaluate and several of them are possibly sidelobes. The theoretical beamforming resolution of the Delay & Sum algorithms is approximately 2 m around 1 kHz, considering the used array configuration. The rotor diameter is 2 m, therefore the investigations should be restricted to frequencies higher than 1 kHz, in order to spatially separate sources in the duct. A lower frequency limit of approximately 3 kHz would impose a three times better resolution (according to Sec. 2) and theoretically allow sources to be separately identified across the rotor diameter and also on the surrounding geometry of the duct.

5.2 Effect of the diagonal removal

The Delay & Sum beamforming results can be seen in Fig. 6 with and without diagonal removal of the cross-spectral matrix. The source maps are corresponding to the one-third octave band center frequency of 3150 Hz. As it was mentioned in Sec. 2, the conventional Delay & Sum method is assuming stationary monopole sources, and therefore the source maps can be interpreted by considering that the moving sources are smeared on the maps. The contours of the rotor inner and outer diameters are overprinted on the pictures as well as the indication of the theoretical resolution of the method. Without the diagonal removal algorithm, the source maps show increasing source levels towards the edge of the source map, where the beamforming is made at off axis angles (i.e. closer to grazing angles). This phenomena disappears when diagonal removal is used, indicating that the effect is the result of the auto spectra of the microphone signals. The source of this noise could possibly be the hydrodynamic pressure field of the turbulent flow over the array, and the reverberated acoustic field of the duct could also have a major contribution. In order to decrease the effect of the high level of flow noise, a 30 mm thick foam cover was mounted on the array surface. The measurement results indicate that perhaps the hydrodynamic pressure fluctuations could still have a mayor contribution in the microphone signals. Effective reduction of this hydrodynamic noise contamination can be obtained by the application of a stretched Kevlar® cloth or a fine metallic net in front of the array as is demonstrated in reference [18].

The dynamic range of the plots in Fig. 6 is small, approximately 1.5 -2dB, without diagonal removal. Such a small level of dynamic range indicates that coherent signals measured by the microphones cannot be reliably identified. It is explained in Sec. 2, that the removal of the diagonal might help to increase the dynamic range significantly. The diagonal removal method increases the dynamic range of the maps up to 5-8 dB. The results with DR are plotted with 5 dB range in Fig. 6. The significant decrease of the source levels of the map can be seen as compared to the conventional case with the diagonal in the cross-spectral matrix. This is expected and clearly supports the previous observation, that the diagonal auto spectral elements are dominating the cross-spectral matrix, and are hiding the sources that are better related to the off diagonal components of the cross-spectral matrix. Because of these considerations only the source maps with the DR method are analyzed in the following. The source maps without DR have a sufficient dynamic range that would allow for conclusions to be made regarding the sources.

5.3 The Delay & Sum results

With diagonal removal, the maps (Fig. 7) are free from the increasing level of sources towards the sides of the source map. The source maps do not reveal the acoustics effect of the rotor. The obtained source spots at the one third octave band center frequency of 3150 Hz and position $y = 0$ m and $x = 1.5$

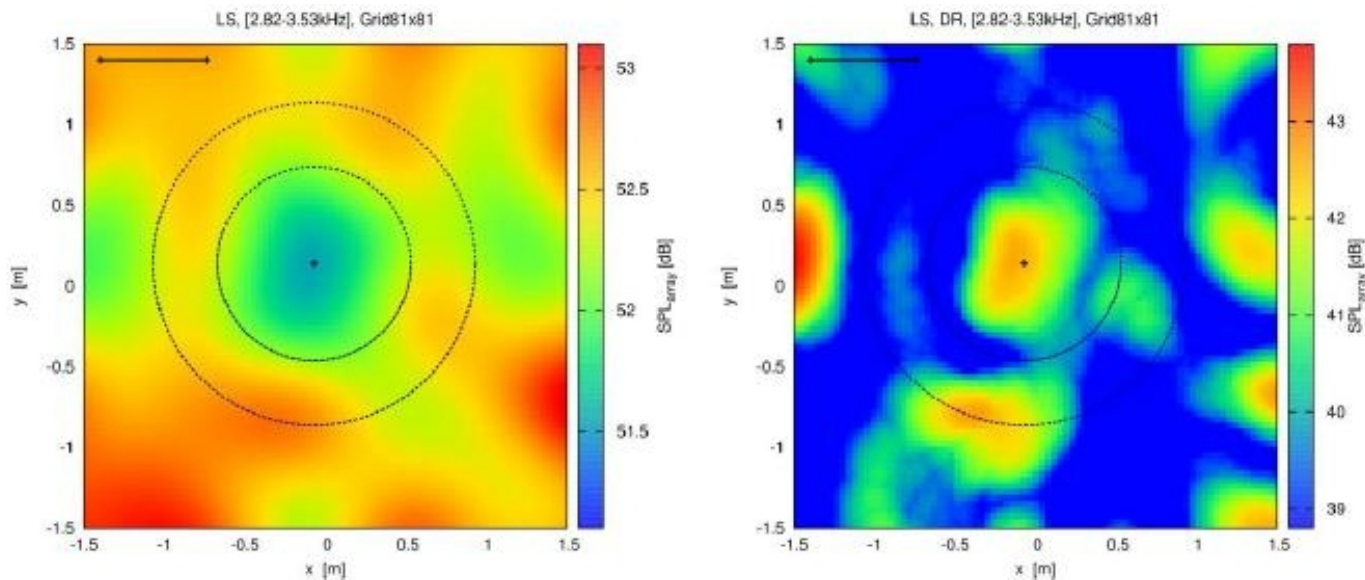


Fig. 6. DS beamforming maps without and with diagonal removal at one-third octave band center frequency of 3.15 kHz

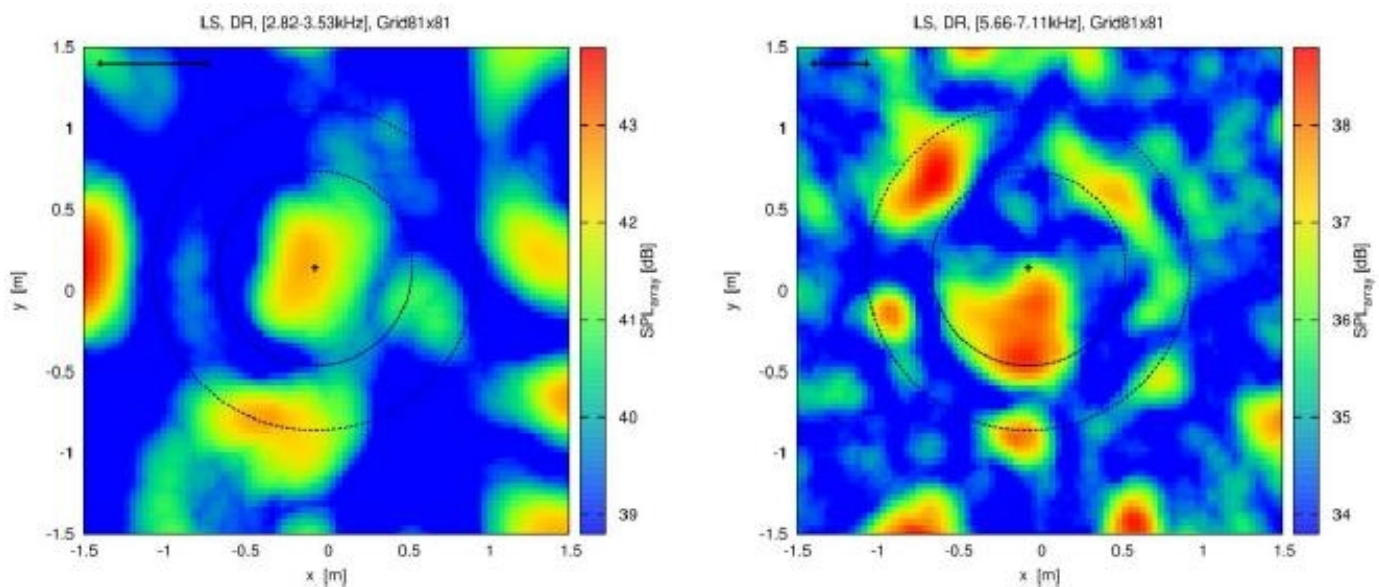


Fig. 7. DS beamforming maps at one-third octave band center frequencies of 3.15 kHz and 6.3 kHz

m can be associated with the bypass doors visible in Fig. 3. These sources do not exist at the one-third octave band center frequency of 6300 Hz. The source spots near the rotor could not be directly associated with any physical obstacles that could explain this type of stationary noise generation, except the possibility of structure born noise from the wind tunnel walls. On the other hand at frequency of 6300 Hz the almost mirror symmetry of the sources respect the vertical mid-plane of the fan ($x = -0.07$ m on the maps) is consistent with the same mirror symmetry of the geometry. Nevertheless an asymmetry can be observed respect the horizontal mid-plane of the fan ($y = 0.14$ m). This probably due the non-symmetrical transition element between the suction duct and the fan (See Fig. 2), which causing a thickened boundary layer of the bottom half of the duct. This implies that the sources can be of aerodynamic nature, if one considers the highly disturbed inlet flows impact onto the rotor-stator configuration. This flow disturbance can be caused

by the open bypass doors and also by the high blockage caused by the microphone array in the test section of the wind tunnel.

5.4 The ROSI results

The rotating sources of the rotor cannot be identified by conventional beamforming with stationary source models. The ROSI algorithm can provide the details regarding the rotating sources, because it uses a rotating source model synchronized to the fan shaft. The center of rotation in the followings graphs is specified at $x_c = -0.07$ m and $y_c = 0.14$ m, according to the nose cone position on the scaled recorded picture.

The results of the ROSI algorithm can be seen in Fig. 8 at various frequencies. Because the acoustic sources on the non-rotating elements of the machine do not correspond to the rotating model, these areas in the pictures are shadowed, and only the rotating annular ring is considered in the analysis. The ROSI model is not expected to localize meaningful sources outside the

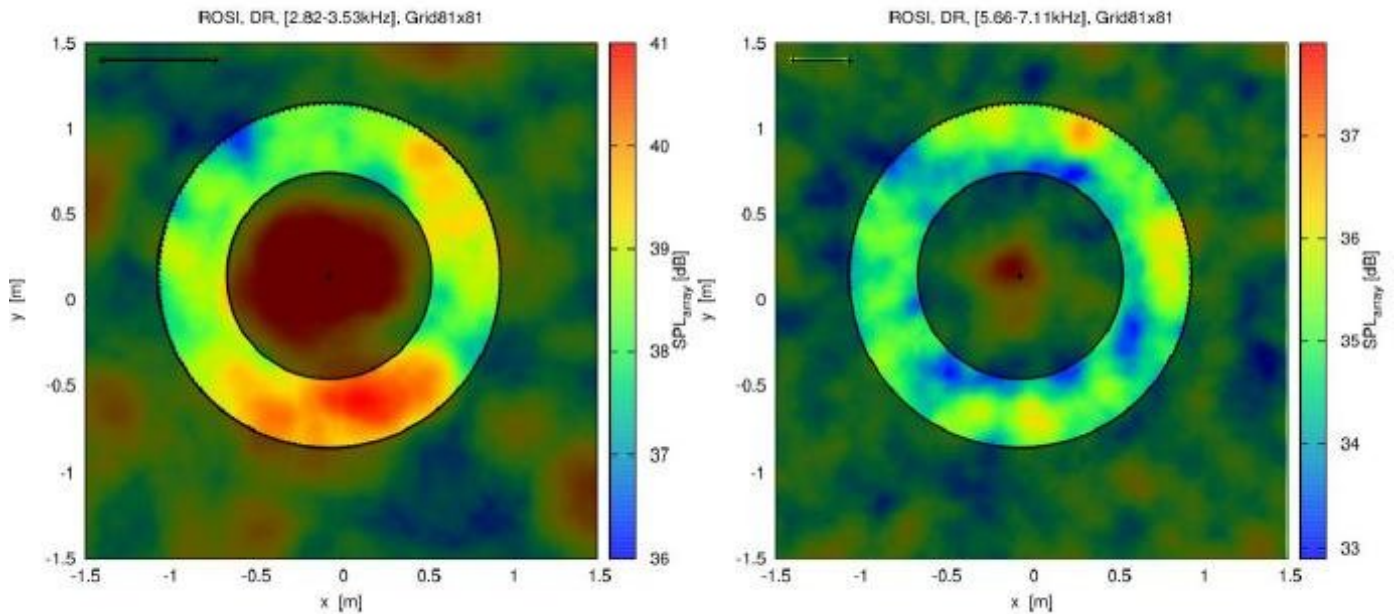


Fig. 8. ROSI beamforming maps at one-third octave band center frequencies of 3.15 kHz and 6.3 kHz

rotating zone. One exception could be the spinning duct modes [19], which can rotate together with the rotor and can generate apparent sources on the beamforming maps outside of the physical rotating zone. This effect is not observed on the presented figures.

The source maps show separated source spots in the annular region of the rotor. Multiple source spots can be observed along the perimeter. The existence of separate source spots instead of a continuous source region is possibly indicates the variation of source strength between the blades and the blade passages. The effect is more pronounced at 6300 Hz. The sources are located around the tips of the rotor blades. The higher source levels around the rotor outer diameter are in agreement with the physical expectation that the noise radiation increases with the flow velocity. Despite this correspondence, the blades cannot be directly identified on the source maps.

The ROSI method gives specialized information regarding the sources on the rotating part of a machine that is not available by conventional beamforming techniques. The conventional beamforming and ROSI methods are recommended to be used simultaneously, used, in order to obtain a global view of noise sources.

6 Conclusions

The acoustic performance of a complex rotating machine in its realistic environment can be obtained by the combination of several analysis methods. General purpose phased array microphone system in combination with dedicated processing algorithms, detailed spectral and simple flow analysis have been used to evaluate acoustic sources of an axial fan. The aim of this paper is such an analysis supported by conventional and rotating source beamforming techniques used in a short timeframe measurement campaign, in a confined industrial environment without any modification of the existing system. In compromise with

that a portable phased array microphone system was installed inside the suction duct.

In order to establish a basis for treating such co-existent multiple noise sources, in-house Delay & Sum as well as ROSI codes have been developed and applied. In future improvement of the Departmental beamforming technique, these in-house built codes will be expected to enable a more flexible and versatile customization to the particular applications, in comparison to commercially available codes

The spectral analysis showed that the broadband noise dominates the acoustic field. The effect of the sampling time on the spectrum was investigated and it was found, that – according to the literature – the necessary minimum length of the averaged microphone data depends on the frequency and should be determined.

Beamforming maps for frequency ranges, which especially sensitive from the viewpoint of human audition, have been presented herein. It was found that, the microphone signals are dominated by the hydrodynamic fluctuations. Therefore the removal of the cross spectral matrix diagonal elements was essentially both the Delay & Sum and ROSI algorithms, to achieve a relevant dynamic range in the acoustic source maps.

The source localization showed that the source strengths has a similar level both on the Delay&Sum and ROSI, this suggest that rotating and stationary sources also exist on the machine. On the Delay&Sum beamforming maps cannot be observed the expected significant circular source pattern in the annular region of the rotor. Characteristic spots on the maps have the same strength, have been assigned to the following elements and effects: suction duct, the opened by pass door, the wake of the array, impacting on the inlet nose cone and the antisymmetry of the transitional element between the suction duct and the fan. The results draw the attention that in an industrial fan layout,

the fan rotor is not necessarily the dominant noise source. Noise originating from other sources may compare or may even dominate over rotor noise.

The ROSI results shows, the rotor noise strength has higher level at higher radius in the higher frequency range of the investigation. This behavior meets the expectations: it is dedicated to the radially increasing blade circumferential speed and blade load. Spanwise increasing blade load is due to the controlled vortex design of the rotor.

Acknowledgement

This study was supported by the Hungarian National Fund for Science and Research under contract No. OTKA K 83807. The authors would like to thank the Hungarian Institute of Agricultural Engineering for providing their wind tunnel for the acoustics tests.

This work has been developed in the framework of the project "Talent care and cultivation in the scientific workshops of BME" project. The project is supported by the grant TAMOP-4.2.2/B-10/1-2010-0009.

The work relates to the scientific programme of the project "Development of quality-oriented and harmonized R+D+I strategy and the functional model at BME". The New Hungary Development Plan (Project ID: TÁMOP-4.2.1/B-09/1/KMR-2010-0002) supports this project.

The authors are also grateful for the useful discussions with János Vad and Csaba Horváth.

References

- 1 Directive 2003/10/EC of the European Parliament and of the Council of 6, Official Journal of the European Union, (February 2003).
- 2 SILENCEproject. silence-ip.org.
- 3 Mueller T, Allen C, Blake WK, Dougherty RP, Lynch D, Soderman P, Underbrink J, *Aeroacoustic Measurements: Chapter 3*, Springer, September 2002. 1 edition.
- 4 Guedel A, Bessac F, *Noise of Ventilation Systems*, (September 2012). In The 10th International Conference on Industrial Ventilation, Paris, France.
- 5 Sijtsma P, Oerlemans S, Holthusen H, *Location of rotating sources by phased array measurements*, (May 2001). In 7th AIAA/CEAS Aeroacoustics Conference.
- 6 Podboy G, Horváth C, *Phased array noise source localization measurements made on a williams international FJ44 engine*, (May 2009). In 15th Aeroacoustics Conference; 30th AIAA Aeroacoustics Conference, Miami, FL, United States.
- 7 Lewis C, Joseph P, *Determining the strength of rotating broadband sources in ducts by inverse methods*, Journal of Sound and Vibration, **295**(3–5), (August 2006), 614–632, DOI 10.1016/j.jsv.2006.01.031.
- 8 Kim Y, Nelson PA, *Estimation of acoustic source strength within a cylindrical duct by inverse methods*, Journal of Sound and Vibration, **275**(1–2), (August 2004), 391–413, DOI 10.1016/j.jsv.2003.06.032.
- 9 Sijtsma P, *Using phased array beamforming to identify broadband noise sources in a turbofan engine*, Technical report, National Aerospace Laboratory NLR, (2009).
- 10 Sijtsma P, *Circular harmonics beamforming with multiple rings of microphones*, 18th AIAA/CEAS Aeroacoustics Conference, (June 2012). Colorado Springs, CO, USA.
- 11 Lars K, *Experimental Aeroacoustic*, (2006). Karman Institute for Fluid Dynamics.
- 12 Mueller TJ, Allen C, Blake W, Dougherty R, Lynch D, Soderman P, Underbrink J, *Aeroacoustic Measurements Chapter 2*, Springer, September 2002. 1 edition.
- 13 Robert P, *10th AIAA/CEAS Aeroacoustics Conference*, (May 2004). Manchester, UK.
- 14 Fenech B, Takeda K, *Beamforming in highly reverberant wind tunnels possibilities and limitations*, 14th international Congress on Sound & Vibration, (2007). Cairns, Australia.
- 15 Vad J, Kwedikha A, Horváth C, Balczó M, Lohász M, Régert T, *Aerodynamic effects of forward blade skew in axial flow rotors of controlled vortex design*, Journal of Power and Energy, **221**(7), (2007), 1011–1023, DOI 10.1243/09576509JPE420.
- 16 Robert P, *Directional acoustic attenuation of planar foam rubber*, (February 2012). In Berlin Beamforming Conference.
- 17 Quayle A, Dowling A, Graham W, Babinsky H, *Obtaining absolute acoustic spectra in an aerodynamic wind tunnel*, Journal of Sound and Vibration, **330**(10), (2011), 2249–2264, DOI 10.1016/j.jsv.2010.10.039.
- 18 Shin H, Graham W, Sijtsma P, Andreou C, Faszer A, *Implementation of a phased microphone array in a Closed-Section wind tunnel*, AIAA Journal, **45**(12), (December 2007), 2897–2909, DOI 10.2514/1.30378.
- 19 Hirschberg A, Reinstra S, *An introduction to aeroacoustics*, (July 2004). Eindhoven University of Technology.